ANALYSIS OF A DEVICE FOR IN-SITU MEASUREMENT OF THE SHEAR MODULUS OF SOIL AT LARGE STRAINS

JOAQUIN MARTI[I] and LUIS RODRIGUEZ-OVEJERO[II]

SUMMARY

This paper presents a method for obtaining the complete shear modulus-shear strain relationship in situ, based on torque and rotation measurements from the Borehole Shear Device (BSD). The method is independent of the constitutive behaviour of the soil.

INTRODUCTION

In order to decide exactly which properties characterise the dynamic behaviour of soil, an assumption must be made first about its constitutive formulation. Only then, the material constants embodied in this formulation can be determined by appropriate tests. Unfortunately, the state-of-the-art is far from a satisfactory and universally accepted constitutive description of soils. As a consequence of this difficulty, notable efforts have been dedicated to the one-dimensional characterisation of cyclic soil behaviour by means of the secant shear modulus, μ, and damping coefficient, β, as a function of the shear strain ε. These two functions are not completely independent; in fact, one can be derived from the other if certain hypotheses (Masing's, for example) are accepted. This paper concentrates on the derivation of the function $\mu(\varepsilon)$.

Present methods for determining $\mu(\varepsilon)$ rely on combinations of field and laboratory procedures. Typically, the shear modulus for small strains ($\leq 10^{-6}$ absolute) is determined in the field by means of a geophysical survey. Then, if the soil is amenable to sampling, specimens are taken for laboratory testing, which usually consists of resonant column tests over the lower range of strains and strain-controlled dynamic triaxial tests or cyclic simple-shear tests at the higher strain levels. The inaccuracies and inconsistencies involved in combined procedures, such as that described above, are well known (e.g. Stokoe et al, 1978). These differences are normally attributed to causes such as soil disturbance, stress relief and consolidation time. The results can be expected to be inconsistent since three different test configurations are used for subjecting three different samples to three different stress paths.

It has therefore become important to develop procedures for determining $\mu(\varepsilon)$ in situ for the complete range of strains of interest (10^{-5} to failure). Rather than examining other attempts in detail, the reader is referred to recent reviews (Anderson and España, 1978; Lodde, 1979). At the time of writing, no existing technology known to the authors fulfills the above requirements.

Two factors are worth considering. First, waves are distorted when propagated in non-linear materials. Hence, wave velocities calculated from arrival times of wave peaks must be expected to introduce errors which increase with the strain level induced. Wave propagation

I Senior Engineer, Dames & Moore, 123 Mortlake High Street, London.
II. Staff Engineer, Dames & Moore, 123 Mortlake High Street, London.

methods are therefore of doubtful value at the higher strain levels. Second, for any device which operates from a borehole, purely geometrical considerations impose a fast decrease of strain levels with distance from the borehole, even for a linear material; this effect is enhanced as the behaviour of the soil becomes progressively non-linear. Consequently, methodologies which use a source and a pickup, face serious drawbacks because of the very non-uniform conditions arising from the rapidly varying strain distribution.

THE BOREHOLE SHEAR DEVICE (BSD)

From the above reasoning, the device sought should operate on the basis of point measurements, as opposed to crosshole, downhole or other source-pickup combinations. Furthermore, it must develop little more than a single shear strain component; compressional strains are particularly unwanted. And, because of the rapidly decreasing strains, disturbance around the borehole must be minimised.

The description of a device resulting from the above constraints is given in another paper presented to this conference (Sidey and Bassett, 1980). The active part of the device is cylindrical, 20 cm in diameter and 50 cm long (see Fig.1). It bores itself into position, thus minimising soil disturbance. It is then capable of expanding radially to recover the pre-existing horizontal stress levels. Finally, it can rotate monotonically or harmonically (at operating frequencies of about 10 Hz) under controlled torque or rotation over a large dynamic range. The analysis described below permits obtaining from such tests the value of the shear modulus for all strains of interest. Further details on what follows can be found in the report presented to the sponsor of this work (Sidey et al, 1979).

ANALYTICAL SOLUTIONS

Static solutions for the rotation of an infinite cylinder in a homogeneous, orthotropic space are easily found for most constitutive laws. In cylindrical coordinates (r,θ,z), equilibrium requires:

$$\tau = \tau_o \, r_o^2/r^2 \qquad (1)$$

where τ is the shear stress $\tau_{r\theta}$ at a distance r from the axis and the subscript $()_o$ refers to the borehole surface.

If the constitutive law in shear is $\tau = f(\varepsilon)$, substitution on the left side of Eq.1 provides, at least implicitly, the strain field. Of special interest later on will be the hyperbolic law (initial modulus μ_i and limiting stress τ_m) which yields the strain field:

$$\varepsilon = \frac{\tau_o}{\mu_i \left[(r/r_o)^2 - \tau_o/\tau_m \right]} \qquad (2)$$

Assuming that geometrical non-linearities are not developed, the θ displacement, u, can be determined by forcing displacements to vanish at infinity:

$$u = -\frac{\tau_m r}{2\mu_i} \ln\left[1 - \frac{\tau_o r_o^2}{\tau_m r^2}\right] \qquad (3)$$

This equation can be modified to produce the torque per unit length, T_1, in terms of the rotation, θ_o, of the cylinder:

$$T_1 = 2\pi r_o^2 \tau_m \left[1 - \exp\left\{-2\mu_i \theta_o / \tau_m\right\}\right] \qquad (4)$$

Dynamic solutions can also be easily obtained for the visco-elastic case; with complex Lamé constants λ, μ and density ρ, the governing equation is:

$$\frac{\partial^2 u}{\partial t^2} = v_s^2 \left[\frac{\partial^2 u}{\partial r^2} + \frac{1}{r}\frac{\partial u}{\partial r} - \frac{u}{r^2}\right] \qquad (5)$$

where $v_s^2 = \mu/\rho$. With its boundary conditions of harmonic input at the cylinder-soil interface and vanishing displacements at infinity, Eq.5 can be integrated to produce steady-state solutions. Noticing that the waves progress outward from the cylinder, Fourier's method of separation of variables yields a harmonic equation in time and a Bessel equation in space. For example, under rotation-controlled conditions:

$$u = \frac{r_o \theta_o}{H_1^{(2)}\left(\frac{\omega r_o}{v_s}\right)} H_1^{(2)}\left(\frac{\omega r}{v_s}\right) e^{i\omega t} \qquad (6)$$

$$T_1 = \frac{2\pi r_o^3 \omega \theta_o \mu}{v_s H_1^{(2)}\left(\frac{\omega r_o}{v_s}\right)} H_2^{(2)}\left(\frac{\omega r}{v_s}\right) e^{i\omega t} \qquad (7)$$

where $H_j^{(i)}$ is the Henkel function ith order and jth kind.

The problem of a finite cylinder harmonically rotating in a bore-hole normal to the fixed or free surface of an elastic half-space was partially solved by Boyer and Oien (1972) using a similar procedure but further complicated by a second space dimension. Although they did not produce strain or displacement fields, they succeeded in relating the torque to the rotation by means of influence coefficients for a wide range of frequencies, depths and aspect ratios.

NUMERICAL ANALYSIS

The computer program selected for the analysis was FINEL (Hitchings, 1976), a general purpose, finite-element system. An axisymmetric, dynamic version based on linear-strain quadrilaterals was used. FINEL had to be modified to accept non-linearities through an iterative secant-modulus procedure. The plane boundaries were provided with

viscous absorbing boundaries while, for the cylindrical boundary, an axisymmetric consistent boundary (of the type presented by Lysmer and and Waas (1972) for plane-strain conditions) had to be developed and implemented. The characteristics of this boundary can be found in Sidey et al (1978). A typical mesh used in the computations is shown in Fig.2.

FINEL was used for reproducing all available close-form solutions for infinite and finite cylinders in elastic and hyperbolic media. Figs.3 and 4 present an elastic example. Following these validations, a number of more complex, non-linear cases were investigated. For example, Figs.5 and 6 correspond to a hyperbolic medium ($\rho = 2 \times 10^3$ Kg/m^3; $\mu_i = 1.8 \times 10^8$ N/m^2; $\tau_m = 5 \times 10^5$ N/m^2). Several conclusions could be reached from the combined numerical and analytical effort:

1) At frequencies less than about 100 Hz, if realistic material properties are assumed, the real part of the dynamic solutions differs little from the static results (e.g. Fig.3) and the imaginary component of the response is very small (Fig.4).

2) Material damping has practically no effect on the solution.

3) Layering does not affect the results significantly. For an elastic material the presence of an infinitely stiff layer 25 cm away from the BSD only modifies the torque by 1%; the distance must decrease to 10 cm for the difference to increase to 10%. The elastic case constitutes an upper bound to possible errors arising from this effect.

4) The ratio between the torques per unit length required to produce identical rotations in finite (length equal five radii) and infinite cylinders was observed to be almost independent of frequency and angle of rotation. In tests on hyperbolic materials, variations were of the order of 2% over the strains of interest.

RECOVERY OF SOIL PROPERTIES FROM FIELD DATA

The torque required to induce a rotation θ_o on a cylinder of large length, h, in elastic soil is:

$$T_{EL} = 4\pi r_o^2 \mu_i h \theta_o \qquad (8)$$

If the cylinder is finite, such torque becomes:

$$T_{EF} = 2\pi r_o^2 \mu_i h \theta_o F_E \qquad (9)$$

where F_E is the influence coefficient first derived by Boyer and Oien (1972). From the conclusions in the former section, F_E can be considered to depend on h/r_o alone. For the present design, $h/r_o = 5$, and for this value, $F_E = 2.31$. In the case of a cylinder in soil with a hyperbolic law, the torque at small dimensionless frequencies $\omega r_o/v_s$ can be expressed as:

$$T_{HF} = \pi r_o^2 h \tau_m \left[1 - \exp\left\{-2\mu_i \theta_o / \tau_m\right\}\right] F_H \qquad (10)$$

As mentioned earlier, the influence coefficient, F_H appeared to be approximately the same for elastic and hyperbolic soil models, even at high strains. It will be assumed for the moment that its value will also be the same for other non-linear soil models, an assumption which will be verified later on.

The operation of the BSD produces a series of corresponding pairs of torque and rotation measurements. When the maximum strains induced are small, the initial modulus μ_i can be determined from Eq.9. For larger strains, in order to obtain the relationship between T and θ_o, the form of the constitutive law must be known. The problem is hence implicit and, in order to solve it, the following procedure is proposed.

Suppose the stress-strain law were hyperbolic. Then, once μ_i is known, a second test at higher amplitude is sufficient to determine τ_m from Eq.10, and hence to determine μ for all values of ε. Indeed:

$$\mu = \frac{\tau}{\varepsilon} = \frac{\mu_o}{1 + \mu_i \varepsilon / \tau_m} \tag{11}$$

where μ_i is already known and τ_m is found solving by iteration the implicit Eq.10, written in the form:

$$\tau_m = \frac{T}{\pi r_o^2 h \left[1 - \exp\left\{- 2\mu_i \theta_o / \tau_m \right\}\right] F_H} \tag{12}$$

A first approximation for τ_m is easily obtained from Eq.10, where the exponential is expanded in series up to second order terms. This is always sufficient for the first iteration due to the good convergence characteristics of Eq. 12. Even if the stress-strain law were not truly hyperbolic, such best fit with a hyperbola would probably be sufficient, particularly for the lower strains . However, in order to avoid imposing a hyperbolic stress-strain law onto the soil, the following improvement to the procedure described has been developed.

The initial modulus μ_i is determined from the lowest pair of T-θ values. The next pairs are used for determining values of τ_m from Eq. 12 up to failure of the soil. Clearly, at each rotation level, the stress-strain law of the soil has been fitted with a hyperbolic law over the range of strains associated with the rotation imposed. The approximation will be less satisfactory as higher strains are developed because a larger portion of the stress-strain law is fitted with the hyperbola. Hence, the value of μ corresponding to a strain ε is best derived using the value of τ_m obtained from the T-θ_o pair with maximum strain ε . Obviously, if the material is hyperbolic, all the τ_m values will be identical.

In summary, based on the torque T required to induce a rotation θ_o, the secant shear modulus μ at each strain level ε, is obtained from Eq. 11, where ε and τ_m are obtained from T and θ_o via hyperbolic relationships.

VERIFICATION OF THE PROPOSED PROCEDURE

In order to verify the adequacy of the procedure described, "numerical field tests" were performed. The soil was given a certain stress-strain law and the BSD was operated numerically, thus producing torque and rotation values. The procedure described above was used to generate $\mu(\varepsilon)$, which was then compared to the original curve. Tests included hyperbolic and non-hyperbolic soils. The tests provide an upper bound of the errors because a real soil will respond according to its true constitutive law, while the numerical soil includes small errors originated by the finite-element procedure.

The first series of numerical field tests were run with a hyperbolic soil. Input data were as follows: $r_o = 0.1m$; $h = 0.5m$; $\mu_i = 1.8 \times 10^9 N/m^2$; $\tau_m = 5 \times 10^5 N/m^2$; $\omega = 100$ rad/sec. From the test at small stains, μ_i was exactly recovered. A second test was run with identical input data except that the displacement was increased to 10^{-4} m. The torque "measured" by the computer program was 9.2×10^{-3} Nm, which yields a value $\tau_m = 4.83 \times 10^5 N/m^2$ when introduced in Eq.12. Fig. 7 shows the input curve together with the one derived from the test. As could be expected, the agreement is excellent since a hyperbolic stress-strain law is being fitted with a hyperbolic approximation.

The true test of the procedure is to verify whether it recovers $\mu(\varepsilon)$ when it does not correspond to a hyperbolic stress-strain law. The same configuration of the above example was used again. An arbitrary stress-strain law was defined; besides the elastic run, tests were performed at displacements of 0.1, 0.5, 1.0 and 3.5 mm. The soil μ-ε curve, the four hyperbolic laws generated by successive approximations and the four points where the hyperbolic laws are used to obtain $\mu(\varepsilon)$ are all plotted together in Fig. 8. The agreement is very reasonable, but it is probably dangerous to use this scheme when the secant modulus is less than 10% of its initial value.

CONCLUSIONS

The generation of dynamic soil properties can be based on two basic observations at the BSD operating frequencies: (1) The real part of the dynamic solutions is closely approximated by the static one; the imaginary part can be neglected. (2) The ratio between the torques (per unit length) required to induce identical rotations in the proposed BSD and in an infinitely long one, depends only on the BSD aspect ratio.

These observations made possible a method for deriving the shear modulus as a function of strain from the field measured values of torque and rotation of the BSD. It can be used for strains corresponding to moduli as low as 10% of its initial value and does not require a presumption of the constitutive behaviour of the soil. The method has been verified in numerical tests and is easily amenable to automation, thus allowing instantaneous tabulation of the moduli-strain values in the field.

ACKNOWLEDGMENTS

This work was funded by the US Air Force under contract No. F29602-78-C-0058; their support is greatly appreciated. Mr. D. Hitchings's help was

invaluable in modifying and running his computer program FINEL.

REFERENCES

ANDERSON, D.G. & ESPAÑA, C. (1978) : "Evaluation of In Situ Testing Methods for High Amplitude Dynamic Property Determination", EPRI Report No. NP-920, Project 769-2 FR.

BOYER, G.R. & OIEN, M.A. (1972) : "Steady Motion of a Torsional Oscillator Clamped in a Borehole", Jour. Sound and Vibr., vol.23, no.2, pp.175-186.

HITCHINGS, D. (1976) : "FINEL Users Manual", Private Document available from Aeronautics Dept., Imperial College of Science and Technology, London.

LODDE, P.F. (1979) : "Wave Propagation Techniques for Determining the In-Situ High-Amplitude Shear Behaviour of Geologic Materials", Air Force Weapons Laboratory, Kirtland, New Mexico, Contract No.F29601-76-C-0015.

LYSMER, J. & WAAS, G. (1972) : "Shear Waves in Plane Infinite Structures", ASCE Jour. Eng. Mech. Div., pp. 85-105.

SIDEY, R.C. & BASSETT, R.H. (1980) : "A Device for In-Situ Measurements of the Dynamic Moduli of Soils at Large Strains", to be presented at the VII World Conference on Earthquake Engineering, Istanbul, Turkey.

SIDEY, R.C., MARTI, J., RODRIGUEZ, L. & WHITE, D. (1979) : "Borehole Shear Device - Feasibility and Preliminary Studies", Air Force Weapons Laboratory, Kirtland, New Mexico, Contract No. F29601-78-C-0058.

STOKOE, K.H., ARNOLD, E.J. & HOAR, R.J. (1978) : "Development of a Bottom-Hole Device for Offshore Shear Wave Velocity Measurement", Offshore Tech. Conf., paper 3210, Houston.

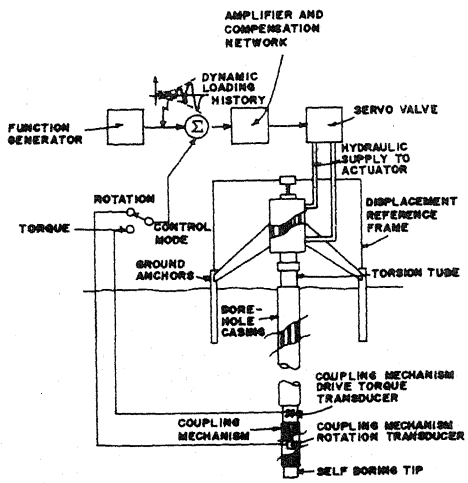

FIG. 1. SCHEMATIC DESCRIPTION OF THE BSD

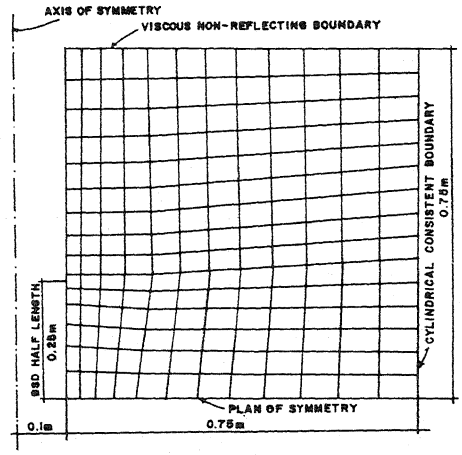

FIG. 2. TYPICAL FINITE ELEMENT MESH USED FOR CALCULATIONS

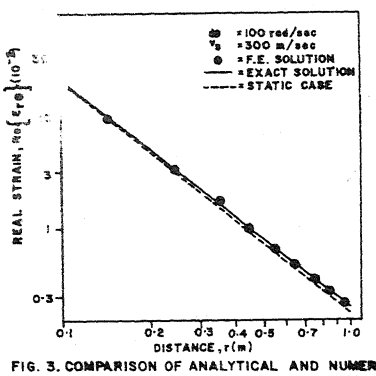

FIG. 3. COMPARISON OF ANALYTICAL AND NUMERICAL ELASTIC SOLUTION FOR LONG CYLINDERS

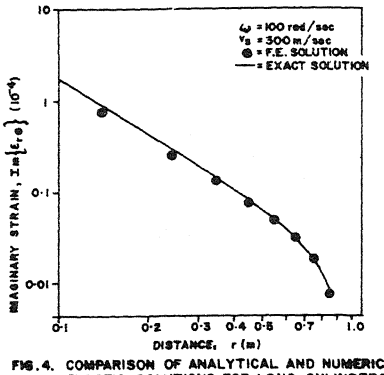

FIG. 4. COMPARISON OF ANALYTICAL AND NUMERICAL ELASTIC SOLUTIONS FOR LONG CYLINDERS

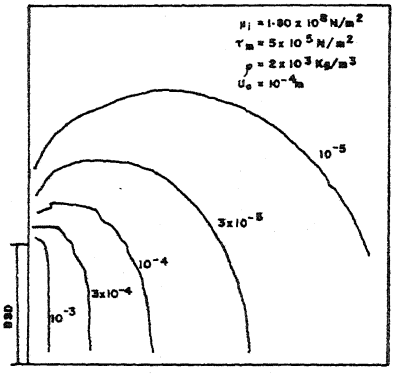

FIG. 5. DISTRIBUTION OF THE REAL PART OF THE $\varepsilon_{r\theta}$ STRAIN FOR A HYPERBOLIC CONSTITUTIVE LAW

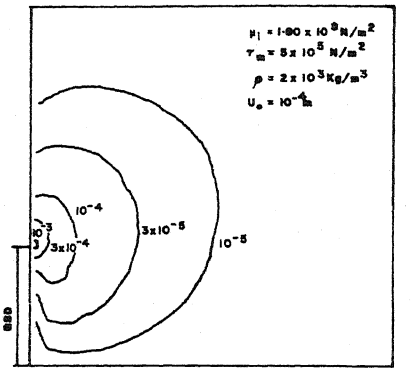

FIG. 6. DISTRIBUTION OF THE REAL PART OF THE $\varepsilon_{\theta z}$ STRAIN FOR A HYPERBOLIC CONSTITUTIVE LAW

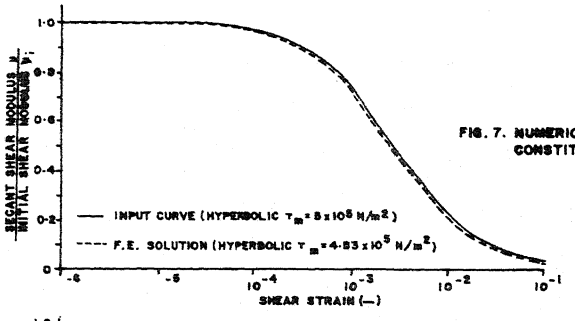

FIG. 7. NUMERICAL REPRODUCTION OF A HYPERBOLIC CONSTITUTIVE LAW

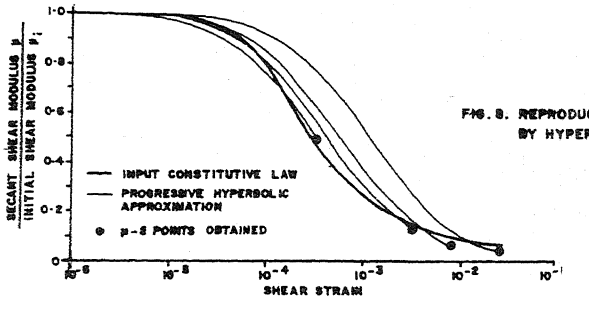

FIG. 8. REPRODUCTION OF THE INPUT CONSTITUTIVE LAW BY HYPERBOLIC APPROXIMATIONS